# Conversion electron Mossbauer spectroscopy and X-Ray diffraction studies of the formation of carbonate-containing green rust one by corrosion of metallic iron in NaHCO3 and(NaHCO3+NaCl) solutions

Abdelmoula Mustapha, Philippe Refait, Sidi El Hassane Drissi, J. P Mihe, Jean-Marie R. Génin

# CONVERSION ELECTRON MÖSSBAUER SPECTROSCOPY AND X-RAY DIFFRACTION STUDIES OF THE FORMATION OF CARBONATE-CONTAINING GREEN RUST ONE BY CORROSION OF METALLIC IRON IN $NaHCO_3$ AND ($NaHCO_3$ + NaCl) SOLUTIONS

M. ABDELMOULA, Ph. REFAIT, S.H. DRISSI, J.P. MIHE and J.M.R. GÉNIN

Laboratoire de Chimie Physique pour l'Environnement, UMR 9992 CNRS-Univ. H. Poincaré

Department of Materials Science, ESSTIN, Université Henri Poincaré

405, rue de Vandoeuvre, F 54600 Villers-les-Nancy, France

**Abstract** : The corrosion of α-iron in 0.1 $mol.l^{-1}$ $NaHCO_3$ solutions, with or without additional NaCl, leads to the formation of a deep-green homogeneous layer which covers the metallic surface. It is analysed by X-ray diffraction (XRD) and conversion electron Mössbauer spectroscopy (CEMS) and proves to be made of carbonate-containing green rust one, $GR1(CO_3^{2-})$, an Fe(II)-Fe(III) hydroxide-carbonate with chemical formula : $[Fe_4^{(II)}Fe_2^{(III)}(OH)_{12}][CO_3 \cdot 2H_2O]$. If left in solution, the green rust layer oxidizes into α-FeOOH goethite. The corrosion process is : Fe ----> $GR1(CO_3^{2-})$ ----> α-FeOOH, without previous formation of ferrous hydroxide, as expected from the Pourbaix diagram of iron in carbonate-containing aqueous media. If removed from the solution and oxidized in the air, the green rust layer oxidizes into a mixture of ferrihydrite or δ-FeOOH, i.e. poorly crystallized hydrated ferric oxide, and of a compound that could be called "ferric green rust" which keeps, in spite of the oxidation of the Fe(II) ions, the original stacking sequence. Iron samples corroded in (0.1 $mol.l^{-1}$ $NaHCO_3$ + 4 $mol.l^{-1}$ NaCl) solutions are also covered with carbonate-containing green rust one layers and the chloride-containing green rust one, $[Fe_3^{(II)}Fe^{(III)}(OH)_8][Cl \cdot nH_2O]$ is not observed even though the $Cl^-$ : $HCO_3^-$ ratio of the solution is as large as 40 : 1.

# INTRODUCTION

Green rusts are Fe(II)-Fe(III) hydroxide compounds. They belong structurally to the pyroaurite group, as first suggested by Stampfl/1/ and Allmann/2/. These minerals consist of alternating positively charged metal hydroxide layers and negatively charged interlayers of water molecules and anions such as $Cl^-$, $SO_4^{2-}$ or $CO_3^{2-}$. The hydroxide layers contain both divalent and trivalent metal cations, the latter being responsible for their positive charge. For instance, the carbonate-containing green rust 1, GR1($CO_3^{2-}$), has the composition : $[Fe_4^{(II)}Fe_2^{(III)}(OH)_{12}]^{2+}[CO_3 \cdot 2H_2O]^{2-}$ /3/, while the chloride-containing green rust 1, GR1($Cl^-$), corresponds to : $[Fe_3^{(II)}Fe^{(III)}(OH)_8]^+[Cl \cdot nH_2O]^-$ /4/.

Green rusts were already identified as corrosion products, on cast iron waterpipes/1,5/ and on steel sheet piles in a harbour/6/. They may play an important role in the corrosion processes of iron, since they are involved in the oxidation of ferrous hydroxides, as transient intermediate compounds between the initial $Fe(OH)_2$ and the final ferric oxyhydroxides, goethite ($\alpha$-FeOOH) and lepidocrocite ($\gamma$-FeOOH). We studied earlier the oxidation of ferrous hydroxide precipitates, for determining several properties of the green rusts, such as their chemical formulae and potentials/3,4,7-9/. The present study is a first approach to point out the role of green rusts in the corrosion of a metallic iron surface. In particular, it is devoted to check the validity of the Pourbaix diagram of iron in carbonate containing aqueous media which was drawn recently /3/. Its adequacy in solutions of pH higher than 10 is proved but remains questionable at lower pH. Thus $NaHCO_3$ solutions of pH around 8 are prepared and the rust layers formed on $\alpha$-iron samples are analysed by X-ray diffraction (XRD) and conversion electron Mössbauer spectroscopy (CEMS).

# EXPERIMENTAL METHOD

*Prepararation of the samples.*

Two types of corrosive solutions are used : 0.1 mol.l$^{-1}$ $NaHCO_3$ solutions, with a pH around 8.4 and (0.1 mol.l$^{-1}$ $NaHCO_3$ + 4 mol.l$^{-1}$ NaCl) solutions, with a pH around 7.4. The metallic samples are 30 mm diameter Armco iron disks. Their surface is scratched with emery cloth and cleaned with alcohol. They are immersed in the corrosive solution, at the bottom of a beaker. They are removed from the solution, quickly dried and analysed by X-ray diffraction (XRD) or conversion electron Mössbauer spectroscopy (CEMS) once completely covered by a homogeneous rust layer. Six samples are prepared. The corresponding experimental conditions are gathered in table 1.

*Conversion Electron Mössbauer Spectrometer (CEMS).*

The decay of the nuclear excited state of $^{57}Fe$ leads to the emission and subsequent resonant absorption of the 14.4 keV photons. These are the photons which are not detected in the Mössbauer effect transmission measurements and correspond to the usual negative peaks of the Mössbauer spectra. They can alikely be used to excite the nuclei which constitute a sample and the principle of conversion electron Mössbauer spectroscopy (CEMS) is based upon the detection of the internally converted electrons emitted after the resonant absorption of $\gamma$-rays takes place. Amongst the occuring events, the emission of K-conversion electrons with a 7.3 keV energy is detected in backscattering experiments and serves for a non-destructive surface analysis. It concerns very thin surface layers at a depth between 50 to 3000 Å. We built an apparatus which allows to combine a cryostat and an in-situ conversion electron Mössbauer spectrometer. The set-up is shown in figure 1. The analysis chamber (bottom of cryostat) is equiped with a Rh-$^{57}Co$ Mössbauer source (50 mCi initial activity) mounted on a velocity transducer. A channeltron is used to detect the 7.3 keV K-conversion electrons. A ultimate vacuum of about $10^{-8}$ torr can be reached in the spectrometer. The cryogenic fluid (liquid helium or liquid nitrogen) taken from the bottom of the reservoir, through a valve to regulate the flow by pumping at the cryostat de-gasing orifice, enters an exchanger which

cools the sample-holder by conduction. A heating resistor wound on the exchanger regulates the temperature. The sample is placed in vacuum and cooled by conduction. All precautions are thus taken to avoid any spurious oxidation of the sample for this backscattering in situ experiment. To change the sample, the cryostat must be warmed up and the vacuum broken.

## EXPERIMENTAL RESULTS

*Samples corroded in 0.1 mol.l$^{-1}$ $NaHCO_3$ solutions.*

Figure 2 shows the XRD pattern of sample 1, left five days in the solution and analysed immediatly after removal. The pattern is constituted of the diffraction lines of three compounds: α-iron (lines denoted by F), α-FeOOH goethite (G) and a green rust one compound (R). These are respectively the initial product, the final product of oxidation, a ferric oxyhydroxide, and the intermediate product between α-Fe and α-FeOOH, an Fe(II)-Fe(III) compound.

All green rust one compounds (GR1s) have the hexagonal structure of the minerals of the pyroaurite group, a structure determined by Allmann/10/. But their lattice parameters differ, depending on the anions present in the compound. For instance, GR1($Cl^-$) has a parameter c about 24 Å /4,11/ while GR1($CO_3^{2-}$) has a parameter c around 22.5 - 22.8 Å /1,3,12,13/. Thus they can be identified by means of XRD. The XRD data from the pattern of figure 2 are compared to those of reference /3/ and gathered in table 2. It can be seen that the green rust formed here is effectively the carbonate-containing compound, as expected. From our experimental data, the values a = 3.174 Å and c = 22.56 Å are computed.

Sample 2 is corroded in the same conditions but analysed by CEMS. The spectrum, measured at 78 K, is displayed in figure 3. The computer-fitting is made of two sextets, $S_1$ and $S_2$, and four quadrupole doublets, $D_1$, $D_2$, $D_3$ and $D_4$. The results are shown in table 3. Sextet $S_1$, with a hyperfine field H of 339 kOe corresponds to α-Fe. Only four out of six peaks are present since the velocity range (-4 to +4 mm.s$^{-1}$) is too narrow. Sextet $S_2$, with a hyperfine

field H of 492 kOe corresponds to goethite (only two out of six peaks are present). The doublets $D_1$, $D_2$ and $D_3$ are those usually found for GR1s /3,14,15/. $D_1$ and $D_2$ are $Fe^{2+}$ doublets, with large isomer shifts IS (1.24 and 1.27 $mm.s^{-1}$) and large quadrupole splittings QS (2.9 and 2.4 $mm.s^{-1}$) while $D_3$ is an $Fe^{3+}$ doublet with smaller IS and QS (0.46 and 0.47 $mm.s^{-1}$). In order to fit correctly the experimental curve, an additional quadrupole doublet $D_4$ has to be used. Its hyperfine parameters IS = 0.47 $mm.s^{-1}$ and QS = 0.98 $mm.s^{-1}$ indicate that it corresponds to a ferric state.

Samples 3 and 4 are also corroded in a 0.1 $mol.l^{-1}$ $NaHCO_3$ solution but immersed under only 1 mm of solution in order to have accelerated corrosion rates. After 21 hours in solution, both samples are covered with an homogeneous green layer. Sample 3 is then removed and the rust layer analysed whereas sample 4 is maintained in solution. The XRD pattern of sample 3 (Fig. 4) displays only the lines of α-Fe and those of GR1($CO_3^{2-}$) which lattice parameters are again found to be : a ≈ 3.175 Å and c ≈ 22.55 Å. After nine more days in solution, sample 4 is covered by an homogeneous ochre layer. The XRD pattern of figure 5 reveals that it is made of α-FeOOH goethite which proves to be the end product of the corrosion process.

*Oxidation of the samples after removal from the solution.*

Sample 1, once corroded in an 0.1 $mol.l^{-1}$ $NaHCO_3$ solution and analysed by XRD, is left one month in the dry atmosphere of the laboratory. The deep-green corrosion layer turns to brown and is analysed by XRD. The pattern is presented in figure 6. It is measured in the same conditions as those chosen for the first pattern of sample 1 (fig. 2), for comparison. The iron (F) and goethite (G) lines have approximately the same intensities in each case. On the contrary, the intensity of the GR1 diffraction lines decreases drastically. In fact, only the main line $R_{003}$ remains clearly noticeable. It corresponds to an interplanar distance $d_{003}$ = 7.34 Å, while the minute $R_{006}$ peak gives $d_{006}$ = 3.67 = (7.34)/2 Å. The lattice parameter c of the compound is equal to 22.02 Å, a value lower than that previously observed, 22.56 Å. Finally, a broad line designated by a question mark is noticeable at θ = 20.65° and corresponds to

d = 2.54 Å. It can be attributed to the (101) line of ferrihydrite, 5 $Fe_2O_3$ • 9 $H_2O$ /16/ or to the (100) line of δ-FeOOH /11,17/.

*Samples corroded in (0.1 mol.l$^{-1}$ $NaHCO_3$ + 4 mol.l$^{-1}$ NaCl) solutions :*

Samples 5 and 6 are left 14 days in the (0.1 mol.l$^{-1}$ $NaHCO_3$ + 4 mol.l$^{-1}$ NaCl) solution and analysed by XRD (Fig. 7) and CEMS at 78 K (Fig. 8), respectively.

In the XRD pattern, along with the α-Fe lines (denoted by F) and NaCl lines (H), the main lines (R) of a GR1 compound are observed. Note that the (00m) lines of green rust are abnormally intense while the (110) line is not observed, indicating that the micro-crystallites are preferentially orientated with their (00m) planes parallel to the iron surface. From the data given in table 4, the lattice parameters of the green rust are computed to be a = 3.174 Å and c = 22.74 Å. This value of the parameter c is characteristic of GR1($CO_3^{2-}$); GR1($Cl^-$) is not obtained.

The CEMS spectrum (Fig. 8) shows the sextet ($S_1$) of α-iron (with only four out of six peaks) and the three doublets $D_1$, $D_2$, $D_3$ of GR1. As for sample 2, an additional ferric doublet $D_4$ is used, and its parameters are computed to be again IS about 0.47 mm.s$^{-1}$ and QS about 1 mm.s$^{-1}$.

## GENERAL DISCUSSION

*Corrosion of iron in 0.1 mol.l$^{-1}$ $NaHCO_3$ solutions.*

In the previous study devoted to the transformation of ferrous hydroxide $Fe(OH)_2$ into GR1($CO_3^{2-}$) /3/, the chemical formula and the free enthalpy of formation of GR1($CO_3^{2-}$) were established, and the Pourbaix diagram of iron in carbonate-containing aqueous solutions was drawn. This diagram, related to a solution with a concentration of carbonate species of 0.1 mol.l$^{-1}$, is presented in figure 9. GRc designates GR1($CO_3^{2-}$). Note that siderite is not reported in the diagram, since it was not observed. Even though it is the stable phase, it does not form under the considered conditions.

This diagram predicted that in carbonate-containing solutions of pH around 8, such as those considered in the present study, the corrosion process of iron could be summarised as follows :

$$Fe \text{ ----> } GR1(CO_3^{2-}) \text{ ----> } \alpha\text{-FeOOH}$$

In these conditions, no ferrous hydroxide should form in a prior stage (figure 9). This process is effectively observed when iron corrodes in 0.1 $mol.l^{-1}$ $NaHCO_3$ solutions and this confirms that under certain conditions $FeCO_3$ siderite do not form. So it appears clearly that Pourbaix diagrams including green rust compounds are to be used when dealing with aqueous solutions containing a fair amount of anions such as $Cl^-$ /4/, $SO_4^{2-}$ /18/ or $HCO_3^-$ and $CO_3^{2-}$ /3/.

CEMS proves to be a suitable method for identifying a green rust one compound at the surface of an iron sample. It seems however impossible to determine the exact nature of the GR1 compound, i.e. to distinguish $GR1(CO_3^{2-})$ from $GR1(Cl^-)$. According to our previous works/4,14,15,19/, GR1 compounds give rise to Mössbauer spectra made of two ferrous doublets, $D_1$ with IS around 1.25-1.30 $mm.s^{-1}$ and QS around 2.85-2.95 $mm.s^{-1}$, $D_2$ with IS around 1.25-1.30 $mm.s^{-1}$ and QS around 2.4-2.7 $mm.s^{-1}$, and one ferric doublet $D_3$ with IS about 0.47 $mm.s^{-1}$ and QS about 0.45 $mm.s^{-1}$. When dealing with stoichiometric green rusts, i.e. when the reaction of formation of the compound is perfectly monitored allowing to analyse the compound before it oxidizes further on, typical $D_1 : D_2 : D_3$ ratio are found. It is 3 : 1 : 2 for stoichiometric $GR1(CO_3^{2-})$ /3,19/ and 2 : 1 : 1 for stoichiometric $GR1(Cl^-)$ /14,15/. Thus the two compounds are theoritically distinguishable. But in the case of natural corrosion products, it is reasonable to assume that non-stoichiometric green rusts are to be analysed. Murad and Taylor studied the oxidation of $GR1(CO_3^{2-})$ by Mössbauer spectroscopy/20,21/. They observed that oxidized non-stoichiometric compounds give rise to an additional ferric doublet with a QS larger than that of $D_3$, around 0.7-1.1 $mm.s^{-1}$. It corresponds to the doublet $D_4$ (see table 3) used to fit the spectrum of our sample which thus proves to be an oxidized non-stoichiometric compound. If $D_4$ is attributed to GR1, the $Fe^{3+}$ amount is about 40% instead of 33% at stoichiometry, leading to the approximate formula :

$$[3.6\ Fe^{(II)}(OH)_2 \cdot 0.4\ Fe^{(III)}OOH \cdot Fe_2^{(III)}(OH)_4][CO_3 \cdot 2H_2O]$$

*Aerial oxidation of GR1($CO_3^{2-}$).*

If maintained in the $NaHCO_3$ solution, GR1($CO_3^{2-}$) oxidizes into α-FeOOH (sample 4) as expected from the Pourbaix diagram. The oxidation process is different if the sample and its GR1 layer are removed from the solution, dried and oxidized in a dry atmosphere. The XRD pattern of the compound thus obtained is essentially made of a line at 7.34 Å, similar to the (003) line at 7.50 Å of GR1($CO_3^{2-}$) and a small line at (7.34)/2 = 3.67 Å, which would correspond to the 006 line. This oxidation process was already observed by Taylor/12/ and corresponds to an in-situ oxidation of the $Fe^{2+}$ ions inside the green rust. The decrease of $d_{003}$ and $d_{006}$ is consistent with the oxidation of $Fe^{2+}$ to the smaller $Fe^{3+}$ cation (ionic radii for $Fe^{2+}$ and $Fe^{3+}$ are 0.78 Å and 0.645 Å respectively/22/). In the case of GR1($Cl^-$), a ferric compound with a structure preserving the original layer stacking is obtained/23/, by oxidizing violently the green rust with hydrogen peroxide $H_2O_2$. This "ferric green rust" is distinguished by relics of the (003) and (006) lines shifted towards lower d values and observed along with δ-FeOOH. The XRD pattern of the compound obtained by aerial oxidation of GR1($CO_3^{2-}$) (figure 6) matches this description.

*Corrosion of iron in (0.1 mol.$l^{-1}$ $NaHCO_3$ + 4 mol.$l^{-1}$ NaCl) solutions.*

CEMS and XRD analyses indicate clearly that a GR1 layer forms in a first stage of the corrosion process, like in $NaHCO_3$ solutions of the type previously studied. As testified by the XRD pattern, this GR1 compound proves to be GR1($CO_3^{2-}$) and not GR1($Cl^-$). It is well known that hydroxides of the pyroaurite class, such as green rusts, exhibit a selectivity of the anion found in the interlayer. It was shown in particular that $CO_3^{2-}$ anions are by far prefered/24/. In the case of green rusts, this preference is linked to the average oxidation number of iron, which is larger in GR1($CO_3^{2-}$) than in GR1($Cl^-$), +2.33 vs +2.25 /3/. This explains why iron can corrode into GR1($CO_3^{2-}$) even if the aqueous solutions have carbonate ions much less numerous than chloride ions.

# CONCLUSION

The corrosion process of iron in a 0.1 mol.l$^{-1}$ $NaHCO_3$ solution of pH around 8.4 is observed to be made of two stages : in the first stage of the reaction, the iron surface covers with a green layer, which proves to be the carbonate-containing green rust one, GR1($CO_3^{2-}$). No previous step corresponding to ferrous hydroxide has been detected. The chemical formula at stoichiometry of the Fe(II)-Fe(III) hydroxide carbonate was recently established as : $[Fe_4^{(II)}Fe_2^{(III)}(OH)_{12}][CO_3 \cdot 2H_2O]$ /3/. In the second stage of the reaction, the GR1($CO_3^{2-}$) layer oxidizes into α-FeOOH goethite, the end product. This aqueous corrosion process of iron matches what is predicted by the Pourbaix diagram of iron in carbonate-containing aqueous solutions/3/ of pH around 8, i.e. Fe → GR1($CO_3^{2-}$) → α-FeOOH, the green rust being an intermediate transient compound between the metallic iron and the "common" rust.

The corrosion of iron in (0.1 mol.l$^{-1}$ $NaHCO_3$ + 4 mol.l$^{-1}$ NaCl) solutions also leads, in a first stage, to a green rust one layer. This compound is the carbonate-containing green rust one. The chloride-containing GR1, $[Fe_3^{(II)}Fe^{(III)}(OH)_8][Cl \cdot nH_2O]$ /4/, is not observed, although the $Cl^-$ : $HCO_3^-$ ratio of the solution is as large as 40 : 1. The corrosion process must be related to the preference of hydroxides of the pyroaurite group for carbonate anions, which gives to GR1($CO_3^{2-}$) an average oxidation number, +2.33, larger than that of GR1($Cl^-$), +2.25, /3,4/. This demonstrates how the properties of green rust compounds can govern the corrosion processes of iron.

## REFERENCES

1. P.P. STAMPFL, *Corros. Sci.*, **9**, 185-187 (1969).

2. R. ALLMANN, *Chimia*, **24**, 99-108 (1970).

3. H. DRISSI, Ph. REFAIT, M. ABDELMOULA and J.M.R. GÉNIN, "Preparation and thermodynamic properties of Fe(II)-Fe(III) hydroxide-carbonate (green rust one), Pourbaix diagram of iron in carbonate-containing aqueous media", submitted to *Corros. Sci.*.

4. Ph. REFAIT and J.M.R. GÉNIN, *Corros. Sci.*, **34**, 797-819 (1993).

5. J.K. BIGHAM and O.H. TUOVINEN, in *Planetary Ecology*, ed. D.E. CALDWELL et al., 239-250, Van Nostrand Reinhold (1985).

6. J.M.R. GÉNIN, A.A. OLOWE, B. RESIAK, N.D. BENBOUZID-ROLLET, M. CONFENTE and D. PRIEUR, in *Marine corrosion of stainless steels : chlorination and microbial effects*, European Federation Corrosion Series n° 10, 162-166, The Institute of Metals, London (1993).

7. A.A. OLOWE and J.M.R. GÉNIN, *Corros. Sci.*, **32**, 965-984 (1991).

8. A.A. OLOWE and J.M.R. GÉNIN, *Hyp. Int.*, **57**, 2029-2036 (1990).

9. Ph. REFAIT and J.M.R. GÉNIN, *Corros. Sci.*, **36**, 55-65 (1994).

10. R. ALLMANN, *Acta Cryst.*, **B24**, 972-977 (1968).

11. J.D. BERNAL, D.R. DASGUPTA and A.L. MACKAY, *Clay Min. Bull.*, **4 /21/**, 15-30 (1959).

12. R.M. TAYLOR, *Clay Miner.*, **15**, 369-382 (1980).

13. I.R. McGILL, B. McENANEY and D.C. SMITH, *Nature*, 29, 200-201, (1976).

14. J.M.R. GÉNIN, D. RÉZEL, Ph. BAUER, A.A. OLOWE and A. BÉRAL, *Electrochem. Methods in Corr. Res., Mat. Sci. Forum*, **8**, 477-490 (1986).

15. J.M.R. GÉNIN, P. BAUER, A.A. OLOWE and D. RÉZEL, *Hyp. Int.*, 29, 1355-60, (1986).

16. F.V. CHUKHROV, B.B. ZVYAGIN, L.P. ERMILOVA and A.L. GORSHKOV, P*roc. Int. Clay Conf. Madrid*, **1**, 397-404, (1973).

17. M.H. FRANCOMBE and H.P. ROOKSBY, *Clay Min. Bull.*, **4 /21/**, 1-14, (1959)

18. A.A. OLOWE and J.M.R. GÉNIN, *Proc. Int. Symp. Sci. Engng.*, CEBELCOR RT297, 363-380, (1989).

19. H. DRISSI, Ph. REFAIT and J.M.R. GÉNIN, *Hyp. Int.*, 90, 395-400, (1994).

20. E. MURAD and R.M. TAYLOR, *Clay Miner.*, **19**, 77-83, (1984).

21. E. MURAD and R.M. TAYLOR, *Ind. Appl. of Mössb. Effect, Hyp. Int.*, 585-593, (1986).

22. R.D. SHANNON, *Acta Cryst.*, **A32**, 751-767, (1976).

23. Ph. REFAIT and J.M.R. GÉNIN, *Corros. Sci.*, **34**, 2059-2070 (1993).

24. A. MENDIBOURE and R. SCHÖLLHORN, *Rev. Chim. Min.*, **23**, 819-827, (1986).

# TABLES

**Table 1 : Preparation of the samples.**

| | Solution | Immersion depth | Immersion time | Analysis | Fig. |
|---|---|---|---|---|---|
| Sample 1 | (a) $NaHCO_3$ | 2 cm | 5 days | XRD | 2 |
| | (b) oxidized one month in air and analysed by XRD | | | | 6 |
| Sample 2 | $NaHCO_3$ | 2 cm | 5 days | CEMS at 78 K | 3 |
| Sample 3 | $NaHCO_3$ | 1 mm | 21 hours | XRD | 4 |
| Sample 4 | $NaHCO_3$ | 1 mm | 10 days | XRD | 5 |
| Sample 5 | $NaHCO_3$ + NaCl | 2 cm | 14 days | XRD | 7 |
| Sample 6 | $NaHCO_3$ + NaCl | 2 cm | 14 days | CEMS at 78 K | 8 |

**Table 2 : XRD data of a sample corroded in a 0.1 mol.l$^{-1}$ $NaHCO_3$ solution (sample 1).**

The (200) line of α-Fe, corresponding to θ = 38.65°, is used to calibrate the experimental spectrum.

| Experimental spectrum (GR lines only) | | | | GR1($CO_3^{2-}$) reference spectrum /1/ | | |
|---|---|---|---|---|---|---|
| θ (°) | $d_{hkl}$ (Å) | $I/I_1$ | $d_{calc}^{(+)}$ (Å) | h,k,l | $d_{hkl}$ (Å) | $I/I_1$ |
| 6.85 | 7.50 | 100 | 7.52 | 0,0,3 | 7.510 | 100 |
| 13.75 | 3.767 | 40 | 3.76 | 0,0,6 | 3.736 | 50 |
| 19.10 | 2.735 | 2 | 2.729 | 1,0,1 | 2.73 | 2 |
| 19.60 | 2.668 | 30 | 2.671 | 0,1,2 | 2.652 | 25 |
| 22.42 | 2.347 | 20 | 2.348 | 0,1,5 | 2.333 | 25 |
| 25.28 | 2.096 | 1 | 2.091 | 1,0,7 | 2.085 | 2 |
| 26.99 | 1.972 | ? | 1.968 | 0,1,8 | 1.961 | 22 |
| 28.45 | 1.879 | 2 | 1.880 | 0,0,12 | 1.88 | 2 |
| 30.88 | 1.744 | 5 | 1.744 | 1,0,10 | 1.736 | 8 |
| 32.98 | 1.644 | 2 | 1.644 | 0,1,11 | 1.637 | 5 |
| 34.33 | 1.587 | 5 | 1.587 | 1,1,0 | 1.579 | 10 |
| 35.20 | 1.553 | 8 | 1.553 | 1,1,3 | 1.547 | 13 |
| 37.73 | 1.463 | 5 | 1.462/1.467 | 1,1,6/1,0,13 | 1.459 | 7 |

(+) Interplanar distances computed with a = 3.174 Å and c = 22.56 Å.

**Table 3 : CEMS (78 K) data of a sample (no. 2 ) corroded in a 0.1 mol.l$^{-1}$ $NaHCO_3$ solution.**

IS = isomer shift, QS = quadrupole splitting, H = hyperfine field and R.A. = relative abundance of components.

| Environment | IS$^{(+)}$ (mm.s$^{-1}$) | QS (mm.s$^{-1}$) | H (kOe) | R.A. (%) | Compound |
|---|---|---|---|---|---|
| S1 | 0.08 | 0 | 339 | 8 | α-iron |
| S2 | 0.47 | -0.24 | 492 | 34 | Goethite |
| D1 | 1.27 | 2.89 | 0 | 30 | GR1 |
| D2 | 1.24 | 2.41 | 0 | 6 | GR1 |
| D3 | 0.46 | 0.47 | 0 | 15 | GR1 |
| D4 | 0.47 | 0.98 | 0 | 8 | |

(+) All isomer shifts are given with respect to α-Fe at room temperature.

Full widths at half maximum were constrained to be equal for each lorentzian line and computed to be 0.30 mm.s$^{-1}$.

**Table 4 : XRD data of a sample (no. 5) corroded in a (0.1 mol.l$^{-1}$ $NaHCO_3$ + 4 mol.l$^{-1}$ NaCl) solution.** (GR lines only)

The (200) line of α-Fe, corresponding to θ = 38.65°, is used to calibrate the experimental spectrum.

| θ (°) | $d_{hkl}$ (Å) | $I/I_1$ | $d_{calc}^{(+)}$ (Å) | h,k,l |
|---|---|---|---|---|
| 6.78 | 7.58 | 100 | 7.58 | 0,0,3 |
| 13.65 | 3.793 | 20 | 3.790 | 0,0,6 |
| 19.53 | 2.678 | 4 | 2.672 | 0,1,2 |
| 22.36 | 2.352 | 4 | 2.353 | 0,1,5 |
| 26.9 | 1.98 | ? | 1.976 | 0,1,8 |
| 28.39 | 1.883 | 2 | 1.895 | 0,0,12 |
| 30.78 | 1.749 | 5 | 1.752 | 1,0,10 |

(+) Interplanar distances computed with a = 3.174 Å and c = 22.74 Å.

**Table 5 : CEMS (78 K) data of a sample (no. 6) corroded in a (0.1 mol.l$^{-1}$ $NaHCO_3$ + 4 mol.l$^{-1}$ NaCl ) solution.**

IS = isomer shift, QS = quadrupole splitting, H = hyperfine field and R.A. = relative abundance of components.

| Environment | IS$^{(+)}$ (mm.s$^{-1}$) | QS (mm.s$^{-1}$) | H (kOe) | R.A. (%) | Compound |
|---|---|---|---|---|---|
| S1 | 0.09 | 0 | 339 | 17 | α-iron |
| D1 | 1.26 | 2.84 | 0 | 38 | GR1 |
| D2 | 1.26 | 2.40 | 0 | 21 | GR1 |
| D3 | 0.48 | 0.49 | 0 | 15 | GR1 |
| D4 | 0.49 | 1.10 | 0 | 4 | |

(+) All isomer shifts are given with respect to α-Fe at room temperature.

Full widths at half maximum were constrained to be equal for each lorentzian line and computed to be 0.35 mm.s$^{-1}$.

## FIGURE CAPTIONS

**Figure 1 :** The Conversion Electron Mössbauer Spectrometer (CEMS).

**Figure 2 :** XRD pattern of sample 1, corroded five days in a 0.1 mol.l$^{-1}$ $NaHCO_3$ solution.
*F, G and R are the lines of α-Fe, α-FeOOH goethite and GR1($CO_3^{2-}$) respectively.*

**Figure 3 :** CEMS spectrum at 78 K of sample 2, corroded five days in a 0.1 mol.l$^{-1}$ $NaHCO_3$ solution.

• • • • : *experimental curve.*

—— : *elementary components.*

- - - - : *global computed curve.*

**Figure 4 :** XRD pattern of sample 3, corroded 21 hours in a 0.1 mol.l$^{-1}$ $NaHCO_3$ solution (1 mm deep).
*F and R are the lines of α-Fe and GR1($CO_3^{2-}$) respectively.*

**Figure 5 :** XRD pattern of sample 4, corroded ten days in a 0.1 mol.l$^{-1}$ $NaHCO_3$ solution (1 mm deep).
*F and G are the lines of α-Fe and α-FeOOH goethite respectively.*

**Figure 6 :** XRD pattern of sample 1, corroded five days in a 0.1 mol.l$^{-1}$ $NaHCO_3$ solution, after aerial oxidation (one month) of the green rust layer.
*F, G and R are the lines of α-Fe, α-FeOOH goethite and green rust respectively.*

**Figure 7 :** XRD pattern of sample 5, corroded 14 days in a (0.1 mol.l$^{-1}$ $NaHCO_3$ + 4 mol.l$^{-1}$ NaCl) solution.
*F, R and H are the lines of α-Fe, GR1($CO_3^{2-}$) and NaCl (halite) respectively.*

**Figure 8 :** CEMS spectrum at 78 K of sample 5, corroded 14 days in a (0.1 mol.l$^{-1}$ $NaHCO_3$ + 4 mol.l$^{-1}$ NaCl) solution.

• • • • : *experimental curve.*

—— : *elementary components.*

- - - - : *global computed curve.*

**Figure 9 :** Pourbaix diagram of iron in carbonate-containing aqueous solution at 25 °C, for a concentration of carbonate species equal to 0.1 mol.l$^{-1}$. (Reference : Drissi et al. /3/)

*GRc designates GR1($CO_3^{2-}$)*

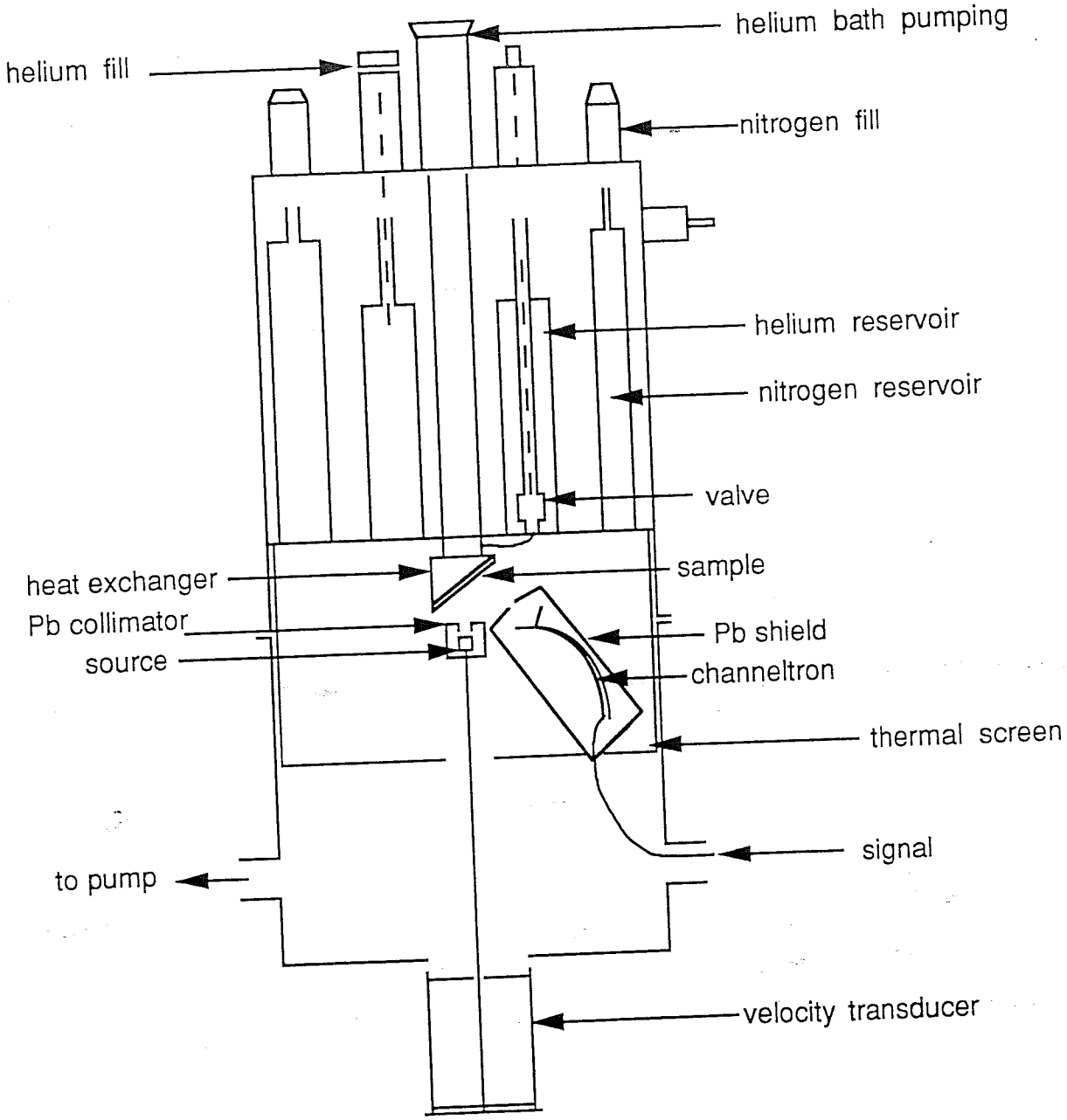
helium bath pumping
helium fill
nitrogen fill
helium reservoir
nitrogen reservoir
valve
heat exchanger
sample
Pb collimator
Pb shield
source
channeltron
thermal screen
signal
to pump
velocity transducer

Fig. 1

Fig. 2

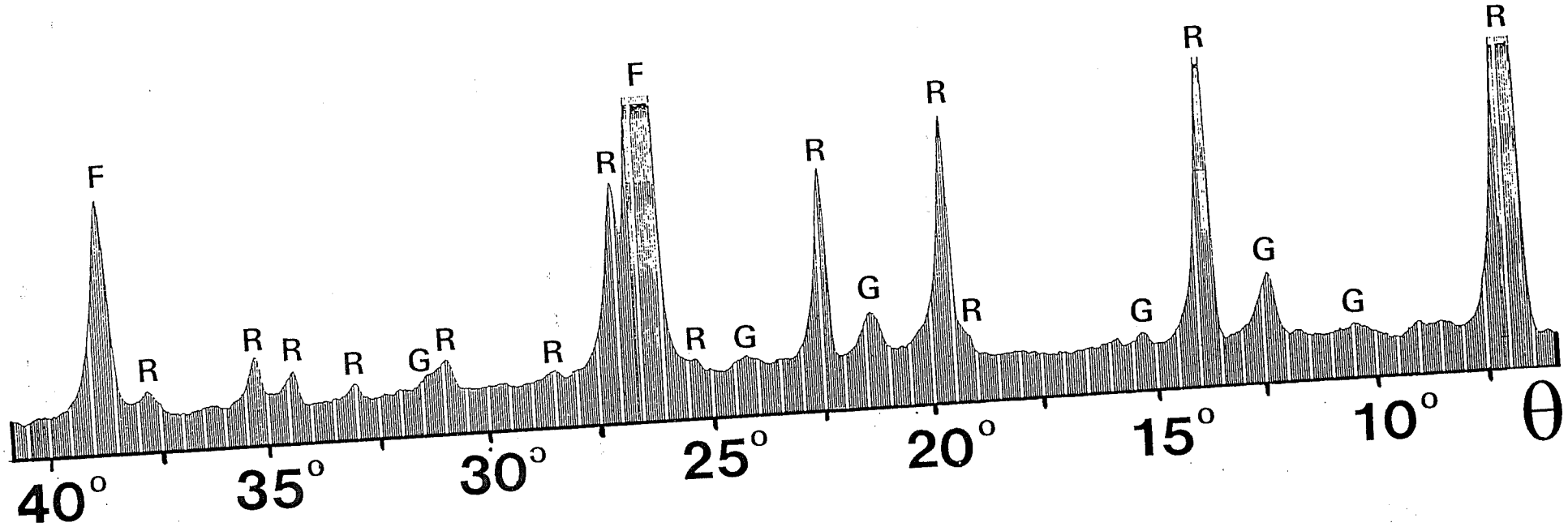

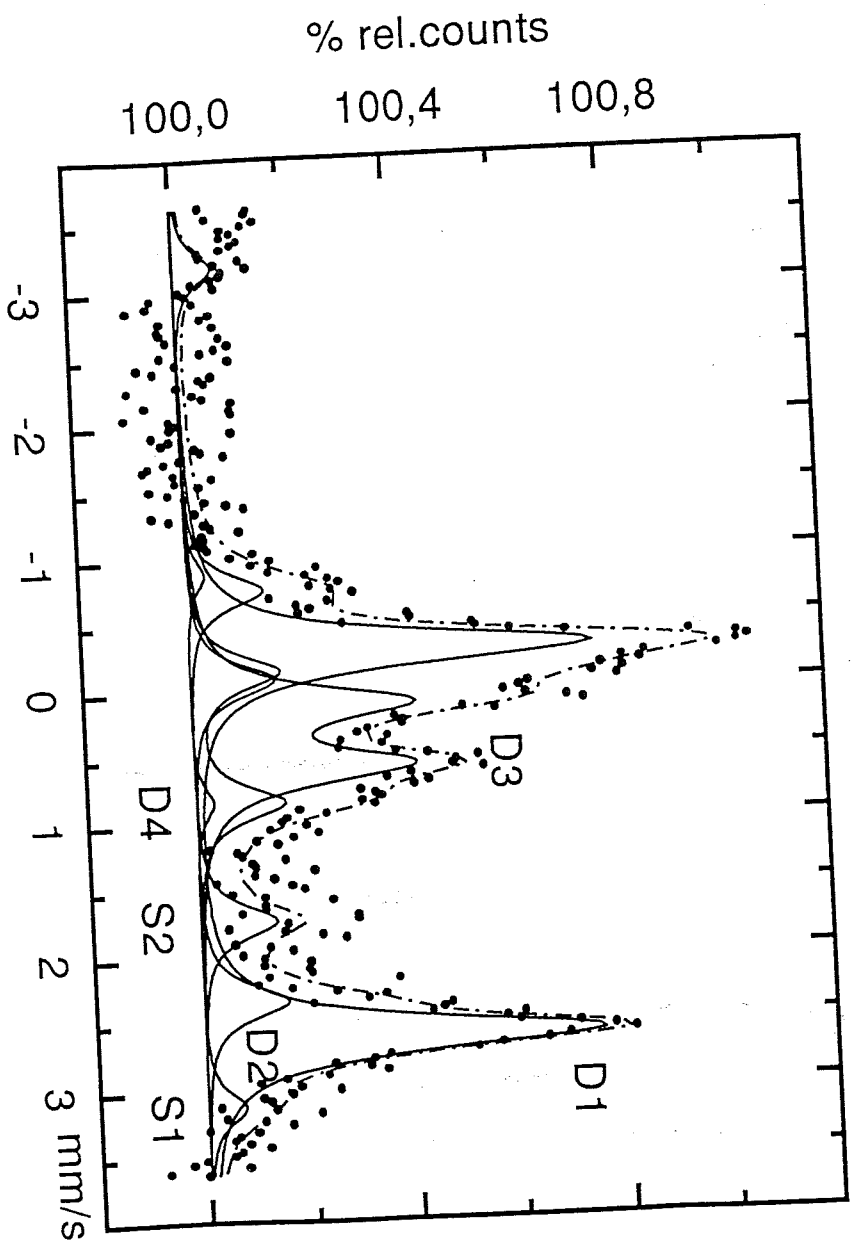


Fig. 3

Fig. 4

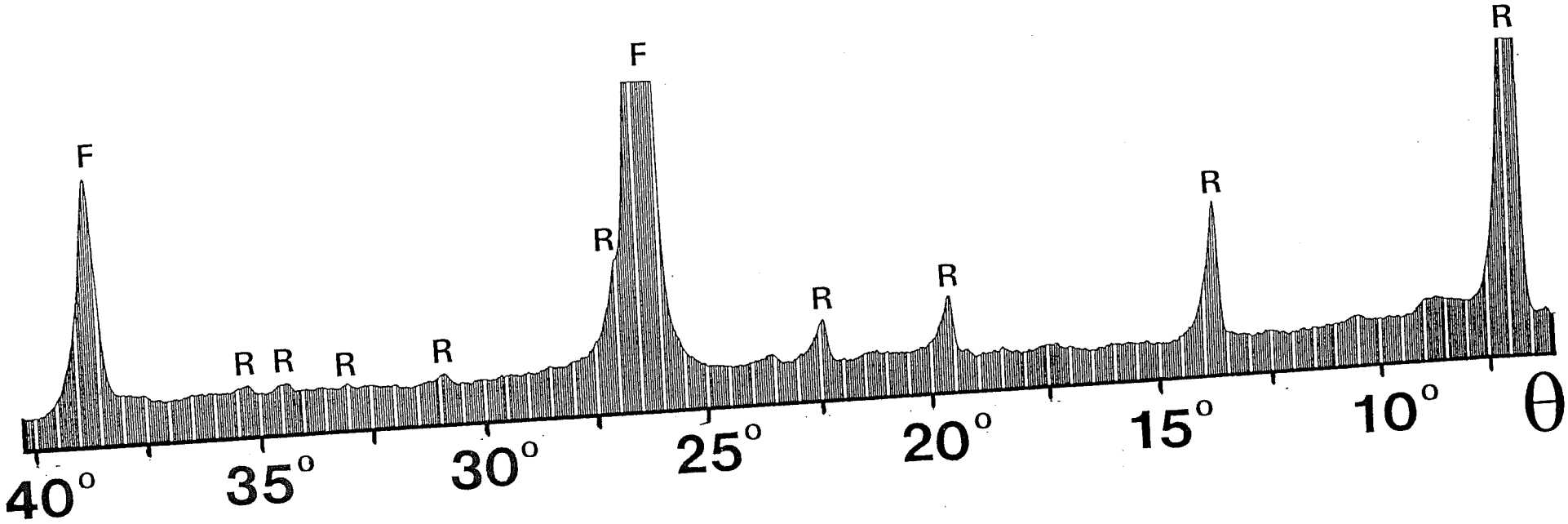

Fig. 5

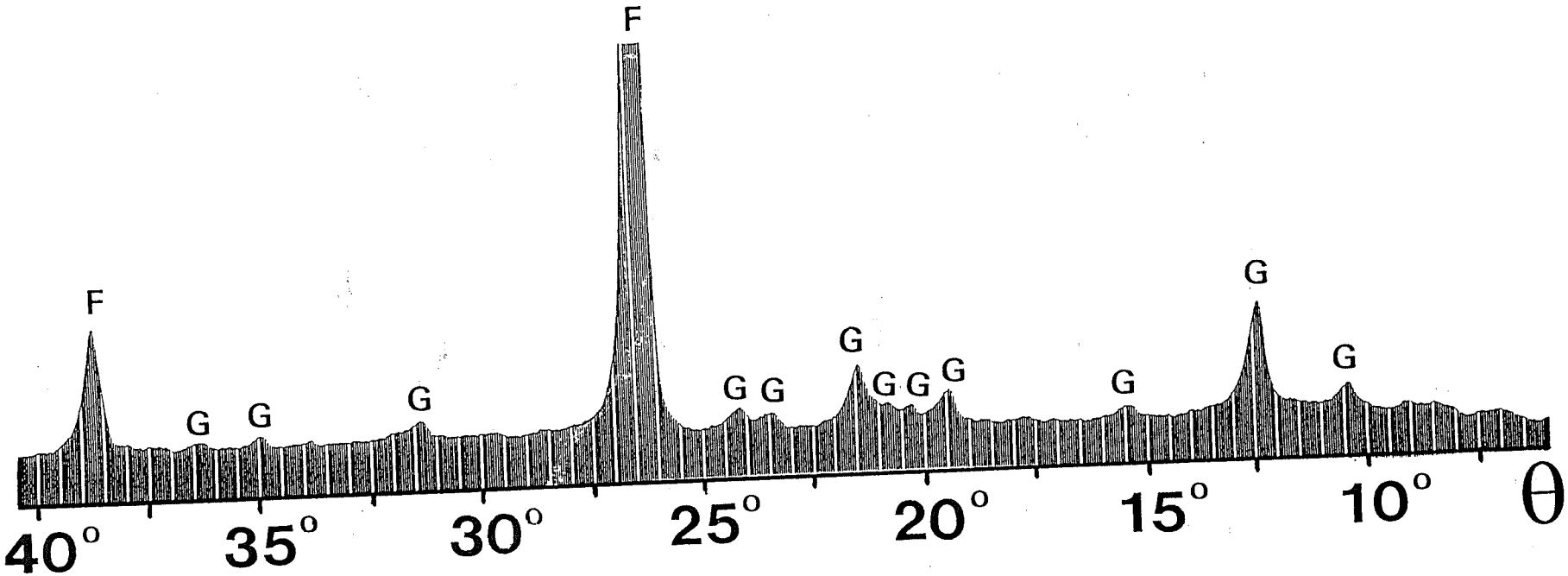

Fig. 6

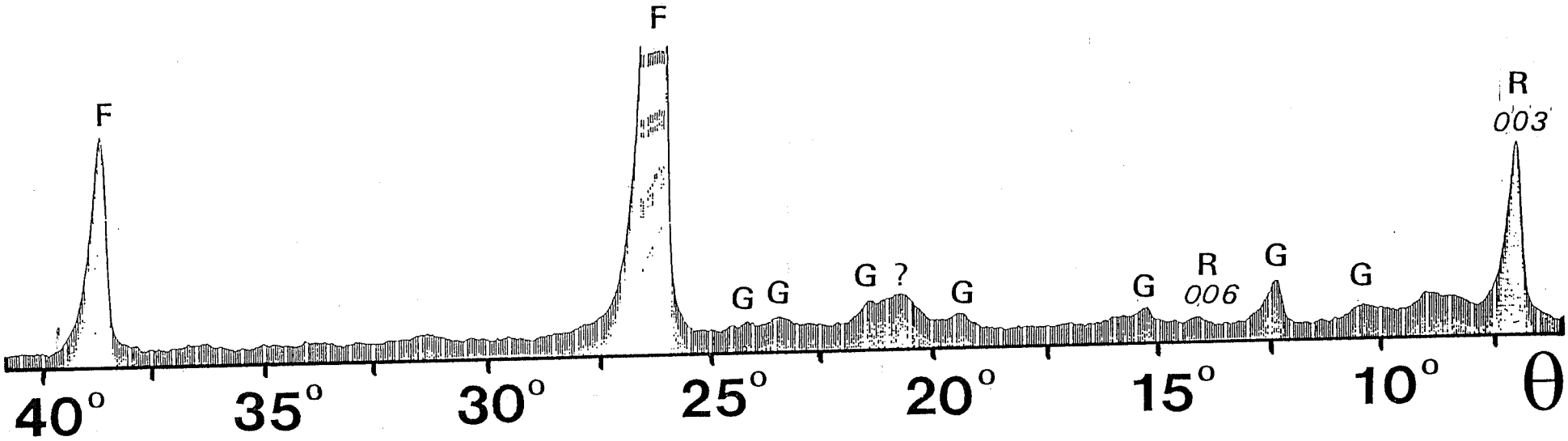

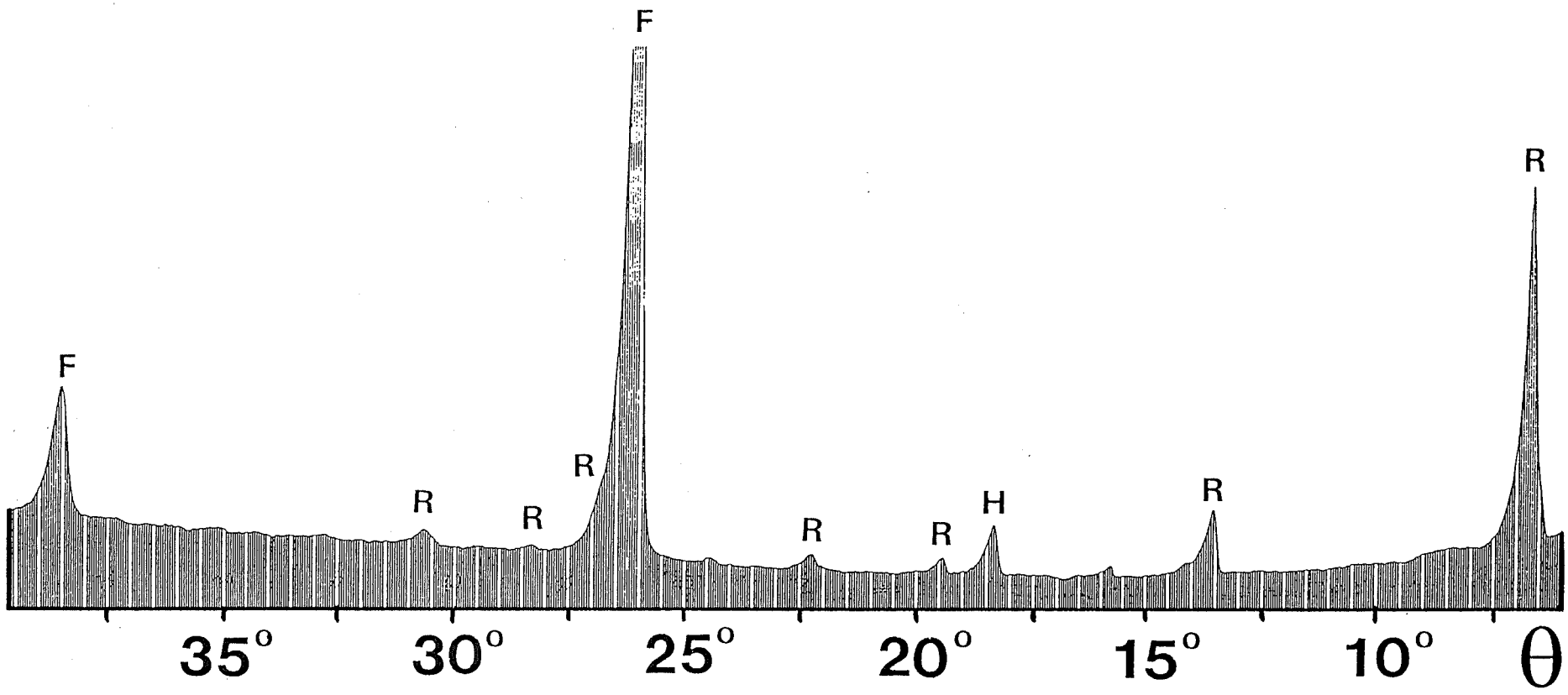
F
F
R
R
R
R
R
H
R
R
35°
30°
25°
20°
15°
10°
θ

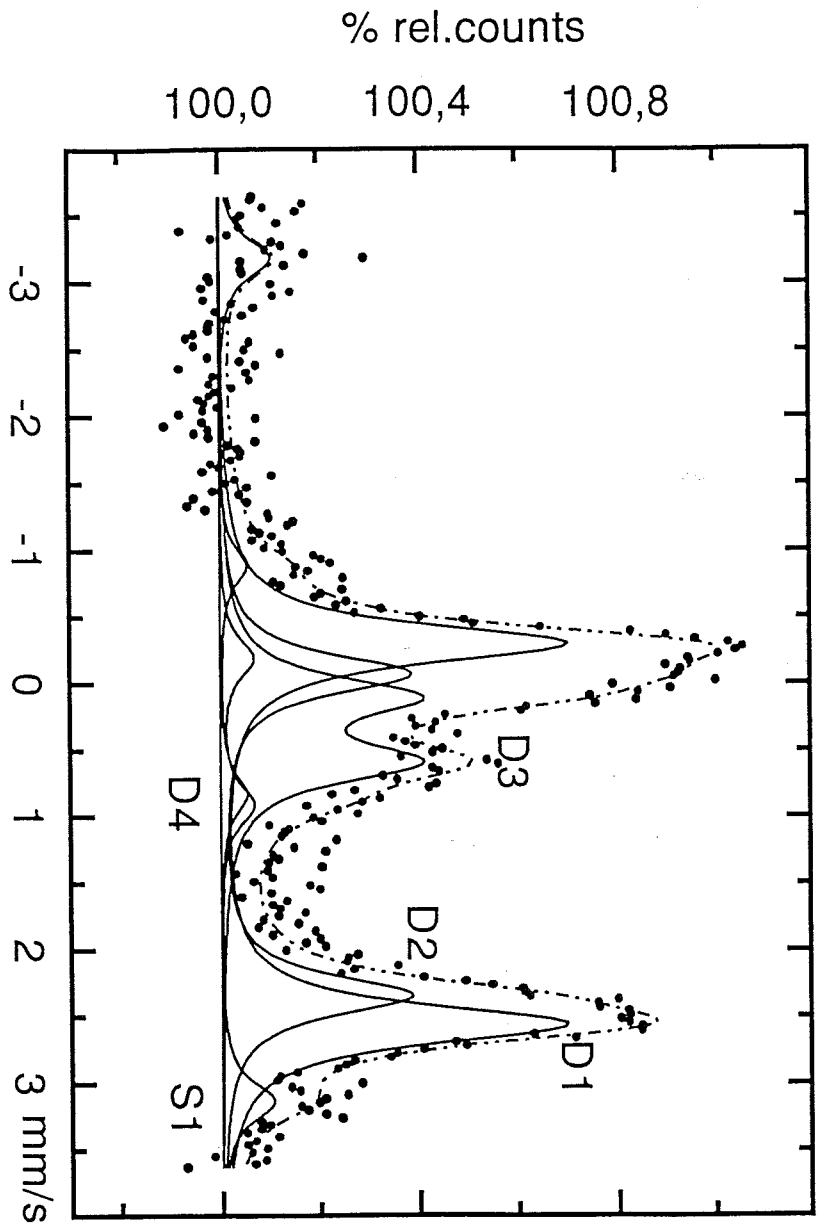


Fig. 8

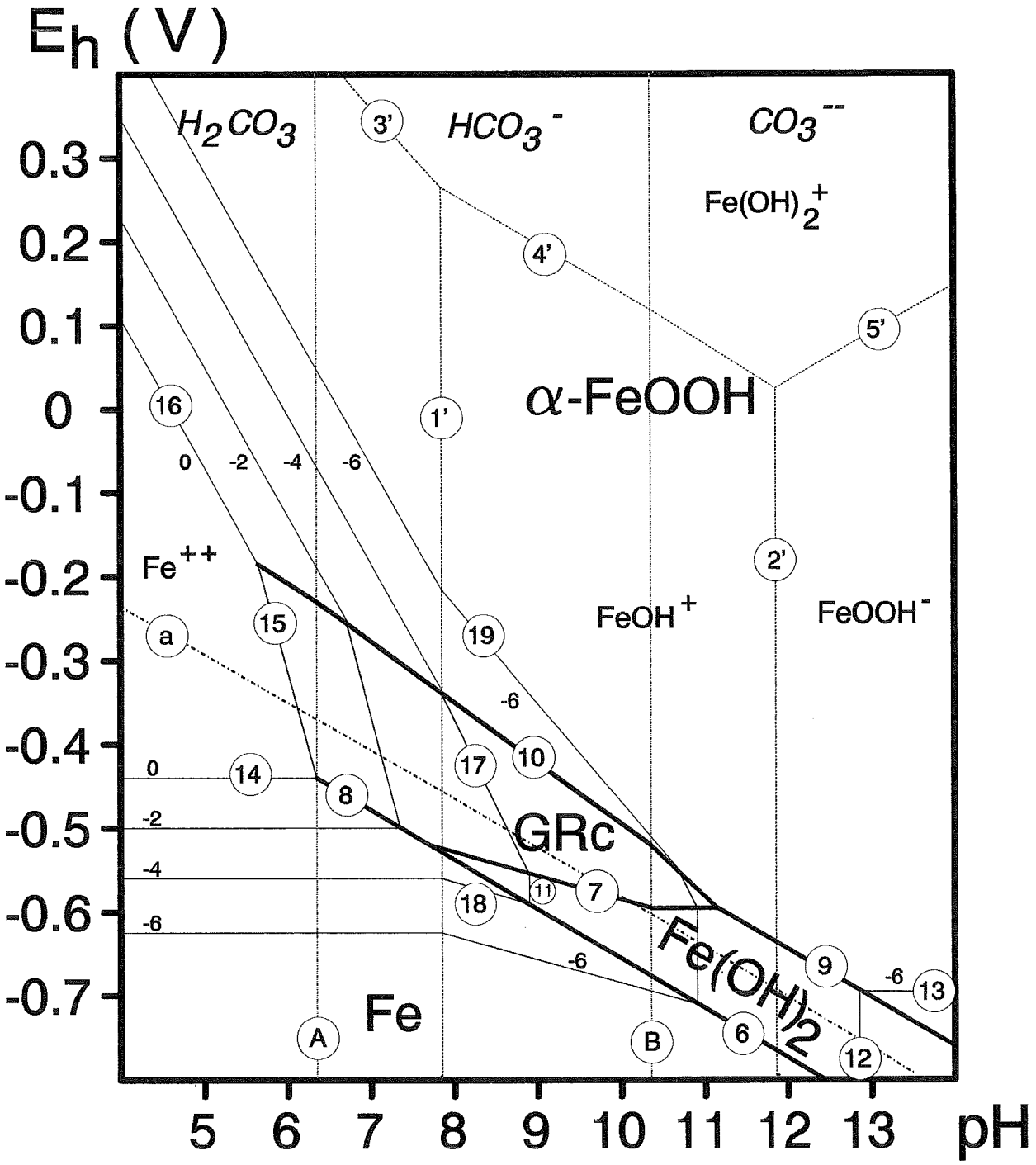
Eh (V)
0.3
0.2
0.1
0
-0.1
-0.2
-0.3
-0.4
-0.5
-0.6
-0.7
H2CO3
HCO3-
CO3--
Fe(OH)2+
α-FeOOH
Fe++
FeOH+
FeOOH-
GRc
Fe
Fe(OH)2
A
B
3'
4'
5'
1'
2'
16
15
19
17
10
14
8
18
11
7
9
13
6
12
a
0
-2
-4
-6
5
6
7
8
9
10
11
12
13
pH

Fig. 9